

## Search for the Muon-Number–Nonconserving Decay $\mu \rightarrow e^+ e^+ e^-$

R. D. Bolton, J. D. Bowman, R. Carlini, M. D. Cooper, M. Duong-van,<sup>(a)</sup> J. S. Frank, A. L. Hallin, P. Heusi, C. M. Hoffman, F. G. Mariam, H. S. Matis,<sup>(b)</sup> R. E. Mischke, D. E. Nagle, V. D. Sandberg, G. H. Sanders, U. Sennhauser,<sup>(c)</sup> R. L. Talaga,<sup>(d)</sup> R. Werbeck, and R. A. Williams  
*Los Alamos National Laboratory, Los Alamos, New Mexico 87545*

and

S. L. Wilson, E. B. Hughes, and R. Hofstadter  
*Hansen Laboratories and Department of Physics, Stanford University, Stanford, California 94305*

and

D. Grosnick and S. C. Wright  
*University of Chicago, Chicago, Illinois 60637*

and

G. E. Hogan<sup>(e)</sup> and V. L. Highland  
*Temple University, Philadelphia, Pennsylvania 19122*  
 (Received 17 July 1984)

A search has been performed for the muon-number–nonconserving decay  $\mu \rightarrow e^+ e^+ e^-$ . No candidate event has been found, the result yielding an upper limit for the branching ratio of  $B_{\mu 3e} < 1.3 \times 10^{-10}$  (90% C.L.). From part of the data taken with a trigger that enhanced  $\mu^+ \rightarrow e^+ e^+ e^- \nu_e \bar{\nu}_\mu$  events, eleven such events were observed. They agree in number and spectra with expectations based on standard electroweak theory.

PACS numbers: 13.35.+s, 11.30.Er, 14.60.Ef

Separate muon, electron, and tau numbers are conserved in the minimal standard model<sup>1</sup> of electroweak interactions with massless neutrinos. However, in many extensions to the standard model<sup>2</sup> separate lepton numbers are not expected to be conserved quantities. Examples of such extensions to the standard model include theories with horizontal gauge interactions, extended hypercolor theories, theories with flavor-changing neutral Higgs bosons, composite models, and theories with new electroweak interactions. The rates in these theories for neutrinoless rare muon decays such as  $\mu^+ \rightarrow e^+ e^+ e^-$  that violate separate-lepton-number conservation generally depend upon undetermined parameters such as mixing angles and heavy particle masses and could be as large as present experimental limits. The present experimental limits on neutrinoless rare muon decays already provide strong constraints on many of the theories that go beyond the standard model. The mass scale being probed is typically in excess of 10 TeV. More sensitive experimental searches for these decays are needed either to discover separate-lepton-number nonconservation or to help eliminate some of these theories.

We report here an improved upper limit for the branching ratio

$$B_{\mu 3e} = \Gamma(\mu^+ \rightarrow e^+ e^+ e^-) / \Gamma(\mu^+ \rightarrow e^+ \nu_e \bar{\nu}_\mu)$$

from the first run with the Crystal Box detector (Fig. 1) in the stopped muon channel at the Clinton P. Anderson Meson Physics Facility (LAMPF). A separated, 26-MeV/c  $\mu^+$  beam was stopped in an elliptical, polystyrene target located at the center of the detector. The target was tilted by 45° with respect to the beam direction; the effective target was 6.7 cm in radius and 52 mg/cm<sup>2</sup> thick. The muon stopping rate was typically  $3 \times 10^5$  s<sup>-1</sup> (average) with a duty factor of 6.8%. The trajectories of charged particles emerging from the target and the energies and times of arrival of electrons, positrons, and photons were measured in the apparatus.

Decay positrons and electrons first traversed a cylindrical drift chamber<sup>3</sup> consisting of eight concentric shells of wires at alternating angles of from 10° to 16° to the axis of the cylinder. The basic drift cell cross section is  $8 \times 10$  mm<sup>2</sup>. The chamber has 728 drift cells. The position resolution of each wire is 140  $\mu$ m (rms). The measured single-track reconstruction efficiency is 95%. There is no applied magnetic field.

Charged particles next traversed a scintillator hodoscope containing 36 counters. Each counter is  $44.5 \times 5.7 \times 1.27$  cm<sup>3</sup>, with a photomultiplier coupled to each end by a light pipe. These counters define the fiducial volume for charged particles. The measured time resolution of each counter is 290 ps

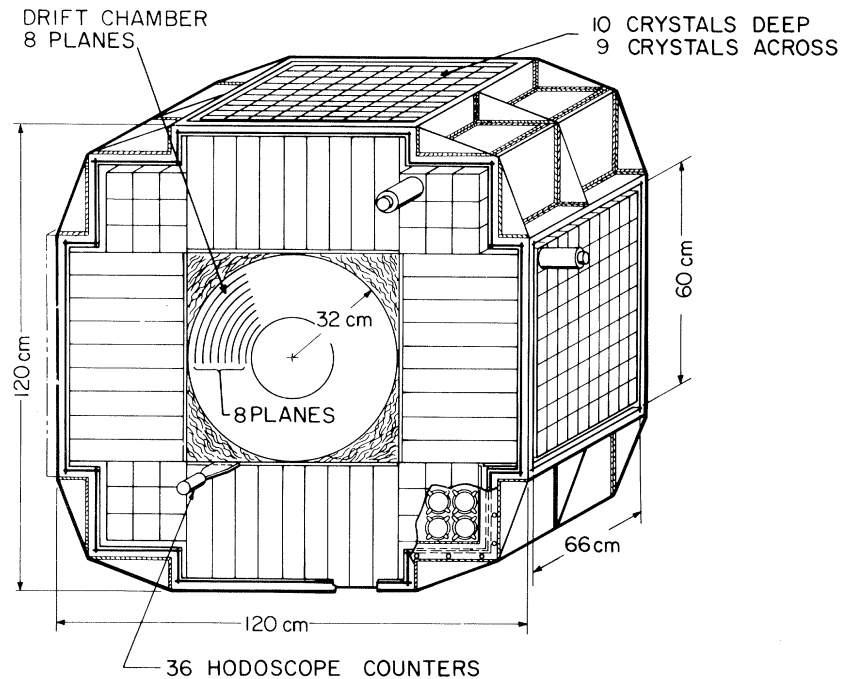


FIG. 1. A schematic diagram of the Crystal Box detector.

full width at half maximum (FWHM). The regions upstream and downstream of the hodoscope are covered by sixteen veto scintillation counters, each measuring  $13.3 \times 23.8 \times 0.3 \text{ cm}^3$ . These counters were used to help distinguish between charged particles and photons.

The outermost part of the detector is an array of 360 NaI(Tl) face crystals,  $6.35 \times 6.35 \text{ cm}^2$  in cross section and 30.5 cm long, plus 36 corner crystals,  $6.35 \times 6.35 \times 63.5 \text{ cm}^3$ . These crystals are packaged in a single hermetically sealed container. Paper wrapping around each crystal provides optical isolation. Each face crystal is coupled to a single photomultiplier while the corner crystals have photomultipliers at both ends. The measured energy resolution function is approximately an asymmetric Gaussian. The FWHM is 6.5% at 130 MeV. Each crystal has its own constant fraction discriminator with a threshold of 5 MeV. The timing resolution of the NaI(Tl) detectors is 1.1 ns (FWHM). The single-particle acceptance in the fiducial area [which assures shower containment in the NaI(Tl) array] is  $\Omega/4\pi = 45\%$ , including finite-target-size effects.

The trigger requirements for a  $\mu \rightarrow 3e$  candidate are as follows<sup>4</sup>: (1) at least three hodoscope-counter signals within 5 ns of each other; (2) at least three nonadjacent-hodoscope-counter signals within 10 ns; (3) a counter topology consistent with  $\mu \rightarrow 3e$  decay; (4) each hodoscope counter participating in the trigger having at least one

discriminator from a NaI(Tl) crystal in the row behind that counter, or in an adjacent row, triggered within 15 ns; (5) for most of the data reported here, at least 80 MeV deposited in the entire NaI array. Approximately 10% of the data were taken without this last requirement to enhance the acceptance for  $\mu^+ \rightarrow e^+e^+e^-\nu_e\bar{\nu}_\mu$  events.

A total of  $2.2 \times 10^{11}$  muons were stopped in the target during the live time of the apparatus. This resulted in  $1.74 \times 10^6$   $\mu \rightarrow 3e$  candidate event triggers. The data written on magnetic tape for each trigger include timing and pulse-height information from every scintillation counter and from each NaI(Tl) crystal having at least 0.1 MeV deposited energy, and timing information from each drift-chamber cell whose discriminator fired.

The absolute gain of each NaI(Tl) crystal was calibrated by use of a Pu- $\alpha$ -Be source ( $E_\gamma = 4.43 \text{ MeV}$ ) and the reactions  $\pi^-p \rightarrow n\pi^0$  ( $\pi^0 \rightarrow \gamma\gamma$ ) ( $55 \leq E_\gamma \leq 83 \text{ MeV}$ ) and  $\pi^-p \rightarrow n\gamma$  ( $E_\gamma = 129.4 \text{ MeV}$ ). The pion data were taken with a liquid hydrogen target replacing the drift chamber. The relative gain of each NaI(Tl) channel was monitored every 2 h by use of a Xe flash tube and fiber optics cables connected to each photomultiplier. Typical gain variations over the course of the run were less than 2%.

The signature for a  $\mu^+ \rightarrow e^+e^+e^-$  event is (a) the three trajectories emerging from a common vertex in the target in time coincidence, (b)  $\Sigma E$ , the

sum of the three energies deposited in the NaI(Tl) array plus the ionization energy losses in other materials, equaling the muon mass, and (c) the vector sum of the three momenta ( $|\Sigma\vec{p}|$ ) being zero.

The main source of triggers was the random coincidence of positrons from three independent ordinary muon decays. These events tend not to satisfy any of the above constraints. Events due to  $\mu^+ \rightarrow e^+e^+e^-\nu_e\bar{\nu}_\mu$ , a process that does not violate separate-lepton-number conservation, have  $\Sigma E + |\Sigma\vec{p}| < M_\mu$  and  $\Sigma E$  generally much less than  $M_\mu$ .

The first analysis pass required that three nonadjacent-scintillator signals occur within a 15-ns interval and that each of these scintillators have behind it a NaI(Tl) clump with at least 10 MeV within a 5-ns interval. A clump is defined as the crystals with the largest local pulse height plus the nearest 24 surrounding crystals. The output of the first pass was  $1.3 \times 10^5$  events.

For the second pass, the drift-chamber information was used to reconstruct tracks that intersected the struck scintillators. The reconstruction program required hits in at least seven of the eight drift-chamber layers for each track. The analysis required three tracks that intersect the target plane with an angle of more than  $3^\circ$ , such that the rms sum of the distances between the three track intersection points on the target (the vertex) is less than 6 cm. Finally, a cut  $\Sigma E + |\Sigma\vec{p}| < 120$  MeV, was imposed. A total of 3112 events survived these cuts.

The third analysis pass tightened the vertex cut after weighting each track-target intersection point

according to the uncertainty in the measurement of that point. The 1.5-ns scintillator timing cut was reimposed after correction of each particle's time-of-flight for the path length from the vertex to the scintillator. This pass reduced the number of events to 83.

The final cuts required that  $\Sigma E + |\Sigma\vec{p}| < 110$  MeV,  $|\Sigma\vec{p}| < 12$  MeV, and that the three scintillator signals occur within a 1-ns interval. No events passed these cuts. The acceptance of the apparatus was calculated with a Monte Carlo program that accurately reproduces the response of the detectors to positrons, electrons, and photons. Electromagnetic showers are simulated with the shower code EGS.<sup>5</sup> The product of the acceptance and detector efficiency for  $\mu \rightarrow 3e$  events, under the assumption of a constant matrix element, is  $(8.5 \pm 0.8)\%$ . We obtain an upper limit of  $B_{\mu 3e} < 1.3 \times 10^{-10}$  (90% C.L.). Bertl *et al.*<sup>6</sup> at the Swiss Institute for Nuclear Research have also recently reported a new upper limit of  $B_{\mu 3e} < 1.6 \times 10^{-10}$  (90% C.L.).

As a check of the performance of the apparatus and the normalization, the portion of the data taken without the total NaI energy requirement ( $2.55 \times 10^{10}$  muons stopped) was analyzed for  $\mu^+ \rightarrow e^+e^+e^-\nu_e\bar{\nu}_\mu$  events. Since these events tend to have a nonzero vector momentum sum, the  $|\Sigma\vec{p}|$  cut was removed. Eleven events passed these cuts. The only significant source of background is random coincidences. We expect less than one background event for this data sample. Background events have a 90% probability to have  $\Sigma E > 80$  MeV: We observe no such events. The Monte Carlo program predicts  $12 \pm 2$  events, using a ma-

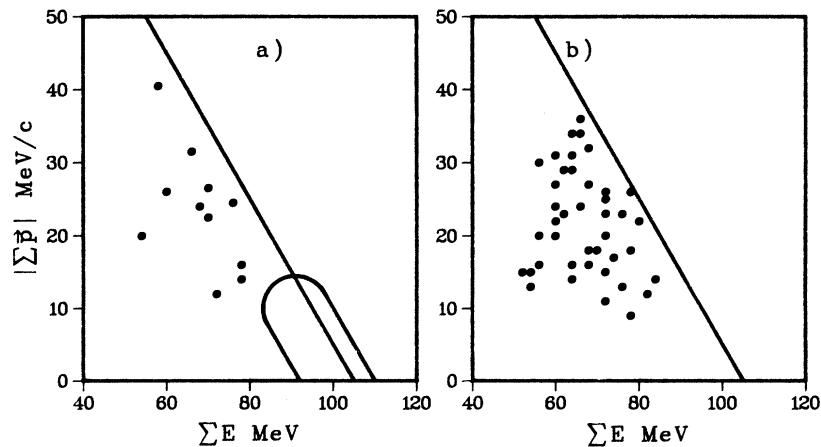


FIG. 2. (a) The vector sum of the momenta for the two positrons and the electron ( $|\Sigma\vec{p}|$ ) vs the sum of their energies ( $\Sigma E$ ) for data events. The sloping line represents the condition  $\Sigma E + |\Sigma\vec{p}| = M_\mu$ . The area enclosed near  $\Sigma E = 100$  MeV,  $|\Sigma\vec{p}| = 0$  contains 90% of Monte Carlo  $\mu^+ \rightarrow e^+e^+e^-$  events. (b) The distribution of Monte Carlo  $\mu^+ \rightarrow e^+e^+e^-\nu_e\bar{\nu}_\mu$  events. The number of Monte Carlo events is not normalized to the number of data events.

trix element based on standard electroweak theory.<sup>7</sup> The measured branching ratio is

$$\frac{\Gamma(\mu^+ \rightarrow e^+ e^+ e^- \nu_e \bar{\nu}_\mu)}{\Gamma(\mu^+ \rightarrow e^+ \nu_e \bar{\nu}_\mu)} = (3.2 \pm 1.0) \times 10^{-7}$$

for  $E_{e^+} > 10$  MeV,  $E_{e^-} > 10$  MeV, and  $\Sigma E > 55$  MeV. The distributions of  $\Sigma E$ ,  $\Sigma E + |\Sigma \vec{p}|$ , vertex, and timing for the data and the Monte Carlo events agree with each other. The agreement of these distributions and of the number of events verifies the validity of the assumed detector resolutions, efficiencies, calibrations, and the beam normalization. Figure 2(a) shows the distribution of  $\Sigma E$  vs  $|\Sigma \vec{p}|$  for the detected  $\mu^+ \rightarrow e^+ e^+ e^- \nu_e \bar{\nu}_\mu$  events and the contour containing 90% of  $\mu^+ \rightarrow e^+ e^+ e^-$  events. Figure 2(b) shows the unnormalized distribution for  $\mu^+ \rightarrow e^+ e^+ e^- \nu_e \bar{\nu}_\mu$  events from the Monte Carlo simulation.

In conclusion, we have searched for the separate-lepton-number-nonconserving decay  $\mu^+ \rightarrow e^+ e^+ e^-$ . We observe no such events and set an upper limit  $B_{\mu 3e} < 1.3 \times 10^{10}$  (90% C.L.). We also observe the decay  $\mu^+ \rightarrow e^+ e^+ e^- \nu_e \bar{\nu}_\mu$ , which does not violate separate-lepton-number conservation, at a rate that agrees with the standard electroweak theory.

A large experiment such as this would not be possible without the contributions of many people. In particular we would like to thank L. Bayliss, H. Butler, S. Chesney, R. Damjanovich, L. G. Doster, M. Dugan, C. Espinoza, T. Gordan, G. Hart, J. McDonough, J. Novak, R. Parks, R. Poe, J. Rolfe, J. Sandoval, H. P. von Guten, and H. Zeman. In addition, we would like to thank the LAMPF staff for their many contributions and L. Rosen for his continuing support of this experiment. This work was supported in part by the U.S. Department of Energy and the National Science Foundation.

<sup>(a)</sup>Present address: Lawrence Livermore Laboratory, Livermore, Cal. 94550.

<sup>(b)</sup>Present address: Lawrence Berkeley Laboratory, Berkeley, Cal. 94720.

<sup>(c)</sup>Present address: Schweizerisches Institut für Nuklearforschung, CH-5234 Villigen, Switzerland.

<sup>(d)</sup>Present address: University of Maryland, College Park, Md. 20742.

<sup>(e)</sup>Present address: Los Alamos National Laboratory, Los Alamos, N. Mex. 87545.

<sup>1</sup>S. L. Glashow, Nucl. Phys. **22**, 579 (1961); A. Salam, in *Elementary Particle Theory: Relativistic Groups and Analyticity* (Nobel Symposium No. 8), edited by N. Svartholm (Almqvist and Wiksells, Stockholm, 1968), p. 367; S. Weinberg, Phys. Rev. Lett. **19**, 1264 (1967).

<sup>2</sup>A brief discussion of many of these extensions can be found in C. M. Hoffman, Los Alamos National Laboratory Report No. LA-UR-84-1327, in Proceedings of the Fourth Course of the International School of Physics of Exotic Atoms on Fundamental Interactions in Low-Energy Systems, Erice, Italy, 31 March–6 April 1984 (to be published); and P. Herczeg and T. Oka, Phys. Rev. D **29**, 475 (1984).

<sup>3</sup>Richard D. Bolton *et al.*, Nucl. Instrum. Methods **188**, 275 (1981).

<sup>4</sup>G. H. Sanders *et al.*, in Proceedings of the Topical Conference on the Application of Microprocessors to High-Energy Physics Experiments, CERN Report No. CERN 81-07, 1981 (unpublished), p. 214.

<sup>5</sup>R. L. Ford and W. R. Nelson, Stanford Linear Accelerator Center Report No. SLAC 210, 1978 (unpublished).

<sup>6</sup>W. Bertl *et al.*, Phys. Lett. **140B**, 299 (1984). The best previous result is  $B_{\mu 3e} < 1.9 \times 10^{-9}$  (90% C.L.) from S. M. Korenchenko, B. F. Kostin, G. V. Mitsel'makher, K. G. Nekrasov, and V. S. Smirnov, Zh. Eksp. Teor. Fiz. **70**, 3 (1976) [Sov. Phys. JETP **43**, 1 (1976)].

<sup>7</sup>D. Yu Bardin, Ts. G. Istahov, and G. V. Mitsel'makher, Yad. Fiz. **15**, 284 (1972) [Sov. J. Nucl. Phys. **15**, 161 (1972)]. The matrix element was evaluated by J. Sapirstein (Stanford Linear Accelerator Center), private communication.